ChemComm

Check for updates

A neutral crystalline imino-substituted silyl radical†

Fiona J. Kiefer, Arseni Kostenko, [ID] Richard Holzner [ID] and Shigeyoshi Inoue [ID] *

The neutral three-coordinated imino(silyl)silyl radical was isolated from the reaction of N-heterocyclic iminosilicon tribromide (I^tBuN-$SiBr_3$) with $NaSi^tBu_2Me$. The radical was fully characterized by X-ray crystallography and electron paramagnetic resonance spectroscopy and supported by quantum chemical calculations.

Since the discovery of the Gomberg radical ($Ph_3C–$), free radicals have been known as one of the most fundamental classes of reactive intermediate species in organic chemistry.[1] Many isolable free radicals have been reported to date.[2] Silyl radicals are a special class of reactive intermediates that have been utilized in various applications in many fields of chemistry.[3] They can be used as reducing agents in organic synthesis by halogen abstraction from organic halides.[4,5] Silyl radicals also form as reactive intermediates in radical hydrosilylation and are used as efficient radical initiators in polymerization reactions.[6] Additionally, they can be used as catalysts, for example in cyclotrimerization of acetylenes.[7] In material chemistry, silyl radicals can be generated on silicon surfaces, allowing for surface modification for specific requirements.[8] Due to the variable applications of silyl radicals, studying their properties, reactivity, and generation methods is very important.

For a long time, silyl radicals could only be observed using electron paramagnetic resonance (EPR) spectroscopy as *in situ* generated, short-lived species. Their existence could be chemically proven by trapping reactions.[9,10] Common methods for generating silyl radicals include hydrogen abstraction,[5] Si–Si bond cleavage (photolysis or thermolysis),[11] one-electron oxidation, or one-electron reduction.[12–14] In 2001, Sekiguchi *et al.* greatly contributed to the field by isolating and fully characterizing the first isolable silyl radical,[15] *i.e.* cyclotetrasilenyl radical **A**

TUM School of Natural Sciences, Department of Chemistry, Wacker-Institute of Silicon Chemistry and Catalysis Research Center, Technische Universität München, Lichtenbergstraße 4, 85748 Garching bei München, Germany.
E-mail: s.inoue@tum.de

† Electronic supplementary information (ESI) available. CCDC 2352376 for **2**. For ESI and crystallographic data in CIF or other electronic format see DOI: **https://doi.org/10.1039/d4cc02167c**

(Fig. 1), in which the spin density is spread over three silicon atoms.[15] This seminal work led to further reports of three-coordinated silyl radicals with the structural motif **B**. The Si radical centre in radicals of type **B** is shielded by sterically encumbering silyl substituents, which prevent radical quenching reactions such as dimerization or hydrogen abstraction. The choice of silyl substituents for silyl radicals utilizes the steric and electronic effects of the bulky silyl groups, causing a planar geometry for **B**-type silyl radicals.[16–18] The silyl groups provide kinetic stabilization and strong σ-donation, increasing the central silicon's electron density.[19,20] Also, NHCs have been utilized for silyl radicals stabilization, *e.g.* radical cation **C**,[21] exploiting NHC σ-donating properties and the spin delocalization into the NHC ring.[22] NHIs (N-heterocyclic imines) present improved donating moieties, and although main-group radical species such as phosphorous[23] and nitrogen-centered radicals stabilized by NHIs have been reported,[24] a neutral, tricoordinate silicon-centered radical (**B**-type) supported by an NHI substituent has not been presented so far. Hailing from disilenes (Si=Si), two isolable silyl radical cations *via* one-electron donation have been reported (**D**-type).[13,18] One of them was obtained from imino(silyl)disilene **1** (Scheme 1), containing the bulky and strongly π-donating ^tBuNHI substituent.[12] However, the disilene structure was maintained, *e.g.* **D-2** (Fig. 1), and no silyl group migration was reported.

Herein we report the generation of a tricoordinate neutral imino(silyl)silyl radical **2**, with two trialkylsilyl substituents and
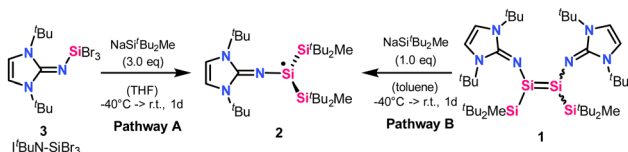

Fig. 1 Selected examples of silyl radicals (**A** and **B**),[15–18] NHC implemented radical cation (**C**),[21] and cationic silyl radicals from disilenes (**D**).[12,13]

Scheme 1 Generation of neutral silyl radical **2** *via* reaction pathways A and B.

an NHI moiety. The synthesis of **2** was achieved by the treatment of N-heterocyclic iminosilicon tribromide (**3**) with three equivalents of sodium silanide NaSi^{t}Bu$_2$Me (Pathway A, Scheme 1) or by reacting imino(silyl)disilene **1** with one equivalent of the sodium silanide (Pathway B, Scheme 1). **2** was isolated and fully characterized by X-ray crystallography, EPR spectroscopy, and quantum chemical calculations.

In 2019, our group reported a tricoordinate silyl radical **B-2** containing three bulky trialkylsilyl substituents,[18] which provide sufficient protection to afford moderate stability of the radical species towards air. In recent years, we have reported increased stability of low-valent silicon compounds when implementing bulky silyl and imino substituents.[25] Electropositive silyl groups, here Si^{t}Bu$_2$Me, are sterically demanding, provide kinetic stabilization, and offer strong σ-donation, increasing the electron density at the central silicon atom.[19,20,26,27] NHI substituents, on the other hand, provide strong π-donation, weak σ-donation, rigid geometry, and thermodynamic stabilization. A combination of both substituent effects afforded thermally stable imino(silyl)disilenes by our group in 2021.[20] One-electron oxidation of imino(silyl)disilene **1** yielded a relatively air-stable radical cation **D-2**.[20]

Upon studying the reactivity of imino(silyl)disilene **1** we found that it reacts with CO to form a three-coordinate neutral imino(silyl)silyl radical **2**, shown in Scheme 1. Carbon monoxide has previously been utilized as a reducing agent, *e.g.* in organic chemistry[28] *via* osmium,[29] iridium,[30] rhodium-based catalysts,[31] or deoxygenation reaction.[32] Synthetically, a toluene solution of imino(silyl)disilene **1** was exposed to 1 bar of carbon monoxide at −40 °C. After 30 minutes, a change of color from deep red (the color of imino(silyl)disilene **1**) to translucent orange was observed. After one day at room temperature, the subsequent extraction with *n*-hexane and recrystallization afforded yellow crystals in 8% yield, which were later identified as the silyl radical **2**, and fully characterized by EPR spectroscopy, X-ray crystallography and quantum chemical calculations (see below). Similar reactivity was not observed with other Lewis bases (I^{i}Pr$_2$Me$_2$, pyridine, phosphines). Attempts to reproduce the formation of the radical species failed – **2** was not observed by EPR spectroscopy when freshly prepared batches of **1** were treated with CO. Our computational investigations aimed at finding a reasonable pathway of formation of **2** from **1** in the presence of CO were also unsuccessful. After further inspections, we began to suspect that CO is not involved in the reaction leading to the radical species, but rather it causes the decomposition of **1** to unidentified products, which results in discoloration of reaction mixtures. Considering this, as well as the reaction irreproducibility, the computational

results and the very low yield of **2** in the initial reaction of **1** with CO, we concluded that radical **2** might be a by-product in the synthesis of **1**.

To study this assumption, we aimed at reproducing the generation of **2**, and finding a reliable reaction pathway for its preparation, by using only the reagents that are used in the synthesis of **1**. Our attempts were successful, as we found that the treatment of the N-heterocyclic iminosilicon tribromide (**3**) with three equivalents of sodium silanide (NaSi^{t}Bu$_2$Me) leads to the formation of **2** in high yields (Pathway A in Scheme 1). Such approach of silyl radical generation, using sodium silanide as a reducing agent, has been previously reported by Sekiguchi *et al.*[15,16] Experimentally, THF was added at −40 °C to the mixture of solids **3** and NaSi^{t}Bu$_2$Me, and an intensive, deep red color could be observed immediately. After one day, the reaction mixture was dried and extracted with *n*-hexane, giving **2**. The reaction can be readily reproduced on a small scale (37 μmol). Considering the mechanism, we propose that in the reaction of **3** with NaSi^{t}Bu$_2$Me the first two salt metastasis steps form the silylbromide intermediate Si(Si^{t}Bu$_2$Me)$_2$(I^{t}BuN)Br. The bulkiness of the silyl substituents does not allow for the third substitution. Instead, Si(Si^{t}Bu$_2$Me)$_2$(I^{t}BuN)Br is reduced by the third equivalent of NaSi^{t}Bu$_2$Me with the subsequent elimination of NaBr and Me^{t}Bu$_2$Si• radical as a disilane dimer [Me^{t}Bu$_2$Si]$_2$ (observed by ^{1}H, ^{29}Si NMR spectroscopy).

As an alternative pathway, **2** can be obtained by treating imino(silyl)disilene **1** (from which **D-2** can also be obtained) with one equivalent of NaSi^{t}Bu$_2$Me at −40 °C in toluene. After extraction with *n*-hexane, **2** is obtained (Pathway B, Scheme 1), and the formation of **2** was verified by EPR spectroscopy (Fig. S6, ESI†).

The structure of **2** was confirmed and characterized by single-crystal X-ray diffraction (SC-XRD) and X-band EPR spectroscopy (Fig. 2). For the EPR measurement, **2** was dissolved in *n*-hexane ($c = 2 \times 10^{-1}$ M) and measured at room temperature. The spectrum shows a strong signal with g value of 2.0034, spitted into seven lines, in the region similar to that of silyl radical stabilized by cAAC ligands (g = 2.0037).[33] Additionally, satellite signals with a hyperfine coupling constant (hfcc) a = 7.166 mT from
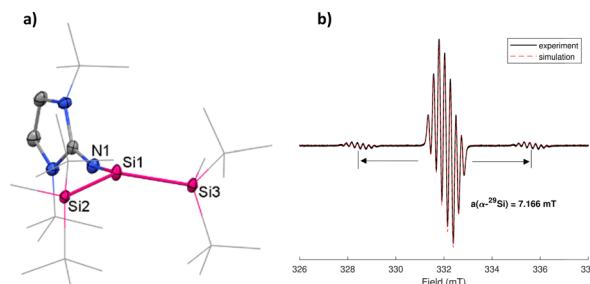

Fig. 2 (a) Molecular structure of silyl radical **2** (left) with thermal ellipsoids drawn at the 30% probability level. Hydrogen atoms are omitted for clarity, ^{t}Bu- and Me-groups are simplified as wireframes. Selected bond lengths [Å] and angles [°]: **2**: Si1–Si2 2.3843(7), Si1–Si3 2.3790(8), Si1–N1 1.676(2), N1–C1 1.280(3), Si2–Si1–Si3 132.98(3), Si3–Si1–N1 108.91(7), N1–Si1–Si2 111.62(7). (b) X-Band EPR spectrum (right) of **2** in *n*-hexane (2×10^{-3} M) at 286 K; (black) experimental, (red) simulation.

Table 1 Experimental and calculated EPR parameters

	g_{iso}	$a(^{14}N1)$	$a(^{14}N2)$	$a(^{14}N3)$	$a(^{29}Si1)$	$a(^{29}Si2)$	$a(^{29}Si3)$
Exp.	2.0034	0.220	0.233	0.201	7.166	0.405	0.033
Calc.	2.0033	0.236	0.247	0.195	6.593	0.372	0.098

Fig. 3 (a) Optimized structure of **2** (iso = 0.04) and the calculated spin density map (purple – positive, orange – negative), at the B3LYP/IGLO-III// r^2SCAN-3c level of theory. Mulliken spin populations of selected atoms: Si1 (0.922), Si2 (−0.040), Si3 (−0.030), N1 (0.106), N2 (0.009), N3 (0.004). (b) Simulated EPR spectrum using the computationally obtained EPR values (Table 1).

the coupling of the unpaired electron with the central α-^{29}Si nucleus are also observed. This α-^{29}Si coupling constant is larger than in a silyl radical bearing three $^tBu_2MeSi$ substituents (a(α-^{29}Si) = 5.80 mT) and thus indicates a higher s-character.[16] The g-value is slightly higher compared to silyl radical cation **D-2** (g = 2.0029).[12] The EPR spectrum in Fig. 2 is comparable to a silyl radical supported by amidinate and imino substituents,[34] while the g-value is comparable to a silyl radical stabilized by cAAC ligands (g = 2.0037).[33] The visible splitting pattern is due to the radical delocalizing to the NHI moiety.[33] Simulation of the EPR spectrum revealed signal splitting pattern resulting from the hyperfine splitting by the three ^{14}N nuclei of the NHI substituent with $a(^{14}N)$ of 0.233 mT, 0.201 and 0.220 m, in addition to the hfccs of the α-^{29}Si nucleus with $a(^{29}Si)$ = 7.166 mT and β-^{29}Si nuclei with $a(^{29}Si)$ of 0.299 and 0.033 mT.

Concurrent with the high s-character deduced from the EPR experiment, SC-XRD analysis of **2** reveals a pyramidalized geometry at the central Si center. A few reported silyl radicals show a planar geometry and sum of bond angles close to 360°.[18,33,34] In **2**, the steric strain of two bulky silyl groups and a bulky NHI ligand is shown in the sum of bond angles being 353.51°, concluding the slightly pyramidal geometry similar to silyl radical cation **C** (Fig. 1). The individual Si–Si bond lengths of Si1–Si2 (2.3843(7) Å) and Si1–Si3 (2.3790(8) Å) are similar to the Si–Si bond length in the disilene **1** precursor (2.3922(7) Å and 2.4001(7) Å) and are shortened in comparison to reported trisilyl-substituted silyl radical **B-2** (2.4533(6) Å and 2.4480(5) Å).[18] Bond distance Si1–N1 (1.676(2) Å) is comparable with that of **1** (1.683(1) Å) and 1.680(1) Å). **2** is susceptible to twinning, which was resolved by applying twin modeling in the refinement process. Its pyramidalized geometry shows a slight disorder of the central Si1 atom of 6.38% occupancy, with a sum of bond angles of 352.42° for the disorder (Fig. S3, ESI†). Disorders in ER$_3$ (E = P) radicals have been reported before.[35] To the best of our knowledge, a silyl radical stabilized by two silyl groups and an NHI ligand has not yet been reported.

To get additional insights into the electronic structure of **2**, quantum chemical calculations were carried out (for additional information about methods see ESI†). The optimized structure of **2** at r^2SCAN-3c level of theory, like the X-ray structure, shows a slightly pyramidal central silicon center with the sum of angles around the Si atom of 352.4° (Fig. 3a). The Mulliken spin population of 0.922 at Si1 indicates the formation of a Si-centered radical. The calculated g value of 2.0033 and the hyperfine coupling constants agree with the experiment (Fig. 3b). The EPR spectrum simulated using the computed g-tensor and the hyperfine coupling constants reproduce the experiment well (Fig. 3b). NBO analysis shows single bonds between the Si atoms with Wiberg bond indexes (WBI) of 0.95 and 0.95 for Si1–Si2 and Si1–Si3, respectively. The Si1–N1 bond with a WBI of 0.83 is significantly polarized toward the nitrogen with 82.6% of the electron density on N1 in the σ(Si1–N1) α orbital and 82.6% in the β orbital. The bonding interaction between C1 and N1 has a multiple bond character with the WBI of 1.53.

In conclusion, our attempts to study the reactivity of imino-(silyl)disilene **1** with carbon monoxide led to the serendipitous isolation of imino-silyl radical **2**. Intentionally, **2** could be obtained *via* two reaction pathways – by reacting I^{t}BuN-SiBr$_3$ with three equivalents of NaSi^{t}Bu$_2$Me (Pathway A) or by treating an imino(silyl)disilene **1** with one equivalent of NaSi^{t}Bu$_2$Me (Pathway B). The neutral, tri-substituted imino-silyl radical **2** was characterized by SC-XRD, EPR spectroscopy, elemental analysis, and quantum chemical calculations. Currently, we are trying to understand the substituent effects of the precursors and looking for ways to generalize the presented methods for obtaining additional related silyl radicals.

Data availability

The data underlying this study are available in the published article and its ESI.†

Conflicts of interest

There are no conflicts to declare.

Notes and references

1 M. Gomberg, *J. Am. Chem. Soc.*, 1900, **22**, 757–771.
2 R. G. Hicks, *Angew. Chem. Int. Ed.*, 2011, **50**, 2213.
3 B. Tumanskii, M. Karni and Y. Apeloig, in *Encyclopedia of radicals in chemistry, biology and materials*, ed. C. Chatgilialoglu and A. Studer, John Wiley & Sons, Chichester, 2012.
4 Z. Rappoport and Y. Apeloig, *The chemistry of organic silicon compounds*, Wiley, New York, 2001.
5 C. Chatgilialoglu, *Organosilanes in radical chemistry*, John Wiley and Sons, Ltd, Chichester, Hoboken, NJ, 2004.

6 J. Lalevée, N. Blanchard, M. El-Roz, B. Graff, X. Allonas and J. P. Fouassier, New Photoinitiators Based on the Silyl Radical Chemistry: Polymerization Ability, ESR Spin Trapping, and Laser Flash Photolysis Investigation, *Macromolecules*, 2008, **41**, 4180–4186.

7 Z. Zhu, C. Wang, X. Xiang, C. Pi and X. Zhou, *Chem. Commun.*, 2006, 2066–2068.

8 C. Chatgilialoglu and V. I. Timokhin, *Silyl Radicals in Chemical Synthesis*, Elsevier, 2008, pp. 117–181.

9 J. K. Kochi, *Free radicals*, vol. I, 1973.

10 J. D. Cotton, C. S. Cundy, D. H. Harris, A. Hudson, M. F. Lappert and P. W. Lednor, *J. Chem. Soc., Chem. Commun.*, 1974, 651.

11 S. Kyushin, H. Sakurai, T. Betsuyaku and H. Matsumoto, *Organometallics*, 1997, **16**, 5386–5388.

12 R. Holzner, A. Porzelt, U. S. Karaca, F. Kiefer, P. Frisch, D. Wendel, M. C. Holthausen and S. Inoue, *Dalton Trans.*, 2021, **50**, 8785–8793.

13 S. Inoue, M. Ichinohe and A. Sekiguchi, *J. Am. Chem. Soc.*, 2008, **130**, 6078–6079.

14 A. Sekiguchi, S. Inoue, M. Ichinohe and Y. Arai, *J. Am. Chem. Soc.*, 2004, **126**, 9626–9629.

15 A. Sekiguchi, T. Matsuno and M. Ichinohe, *J. Am. Chem. Soc.*, 2001, **123**, 12436–12437.

16 A. Sekiguchi, T. Fukawa, M. Nakamoto, V. Y. Lee and M. Ichinohe, *J. Am. Chem. Soc.*, 2002, **124**, 9865–9869.

17 K. Taira, M. Ichinohe and A. Sekiguchi, *Chemistry*, 2014, **20**, 9342–9348.

18 R. Holzner, A. Kaushansky, B. Tumanskii, P. Frisch, F. Linsenmann and S. Inoue, *Eur. J. Inorg. Chem.*, 2019, 2977–2981.

19 V. Y. Lee, *Organosilicon compounds*, Academic Press, Amsterdam, 2017.

20 D. Reiter, R. Holzner, A. Porzelt, P. Frisch and S. Inoue, *Nat. Chem.*, 2020, **12**, 1131–1135.

21 M. Kira, T. Ishima, T. Iwamoto and M. Ichinohe, *J. Am. Chem. Soc.*, 2001, **123**, 1676–1682.

22 H. Tanaka, M. Ichinohe and A. Sekiguchi, *J. Am. Chem. Soc.*, 2012, **134**, 5540–5543.

23 O. Back, B. Donnadieu, M. von Hopffgarten, S. Klein, R. Tonner, G. Frenking and G. Bertrand, *Chem. Sci.*, 2011, **2**, 858.

24 L. Y. M. Eymann, A. G. Tskhovrebov, A. Sienkiewicz, J. L. Bila, I. Živković, H. M. Rønnow, M. D. Wodrich, L. Vannay, C. Corminboeuf, P. Pattison, E. Solari, R. Scopelliti and K. Severin, *J. Am. Chem. Soc.*, 2016, **138**, 15126–15129.

25 D. Wendel, D. Reiter, A. Porzelt, P. J. Altmann, S. Inoue and B. Rieger, *J. Am. Chem. Soc.*, 2017, **139**, 17193–17198.

26 R. Holzner, D. Reiter, P. Frisch and S. Inoue, *RSC Adv.*, 2020, **10**, 3402–3406.

27 C. R. W. Reinhold, M. Schmidtmann, B. Tsumanskii and T. Müller, *Chem. – Eur. J.*, 2021, **27**, 12063–12068.

28 A. A. Tsygankov, M. Makarova and D. Chusov, *Mendeleev Commun.*, 2018, **28**, 113–122.

29 M. M. Vinogradov, O. I. Afanasyev, Y. V. Nelyubina, G. L. Denisov, D. A. Loginov and D. Chusov, *Mol. Catal.*, 2020, **498**, 111260.

30 A. P. Moskovets, D. L. Usanov, O. I. Afanasyev, V. A. Fastovskiy, A. P. Molotkov, K. M. Muratov, G. L. Denisov, S. S. Zlotskii, A. F. Smol'yakov, D. A. Loginov and D. Chusov, *Org. Biomol. Chem.*, 2017, **15**, 6384–6387.

31 V. S. Ostrovskii, S. A. Runikhina, O. I. Afanasyev and D. Eur, *J. Org. Chem.*, 2020, **2020**, 4116–4121.

32 T. Maulbetsch, E. Jürgens and D. Kunz, *Chemistry*, 2020, **26**, 10634–10640.

33 Y. Li, Y.-C. Chan, B.-X. Leong, Y. Li, E. Richards, I. Purushothaman, S. De, P. Parameswaran and C.-W. So, *Angew. Chem.*, 2017, **129**, 7681–7686.

34 S.-H. Zhang, E. Carter, H.-W. Xi, Y. Li, K. H. Lim and C.-W. So, *Inorg. Chem.*, 2017, **56**, 701–704.

35 X. Pan, Y. Su, X. Chen, Y. Zhao, Y. Li, J. Zuo and X. Wang, *J. Am. Chem. Soc.*, 2013, **135**, 5561–5564.